Talanta 88 (2012) 295–302

Contents lists available at SciVerse ScienceDirect

Talanta

journal homepage: www.elsevier.com/locate/talanta

Highly sensitive thrombin detection by matrix assisted laser desorption ionization-time of flight mass spectrometry with aptamer functionalized core–shell Fe_3O_4@C@Au magnetic microspheres

Xueyang Zhang, Shaochun Zhu, Chunhui Deng, Xiangmin Zhang*

Department of Chemistry & Institutes of Biomedical Sciences, Fudan University, Shanghai 200433, China

ARTICLE INFO

Article history:
Received 26 July 2011
Received in revised form
30 September 2011
Accepted 4 October 2011
Available online 31 October 2011

Keywords:
Aptamer
Thrombin
MALDI-TOF
Gold-coated magnetic microspheres
Human serum
Ion oxide

ABSTRACT

Here, we describe a sensitive and specific method for thrombin detection with aptamer functionalized core–shell Fe_3O_4@C@Au magnetic microspheres (Au-MMPs). Firstly, Au-MMPs were synthesized through surface adsorption of gold nanoparticles onto PDDA functionalized Fe_3O_4@C magnetic microspheres. Then, the as-synthesized Au-MMPs were developed as new substrate for immobilization of thrombin binding aptamer (TBA) through easy formation of Au–S bond. After that, the prepared aptamer functionalized Au-MMPs (TBA@Au-MMPs) were used as effective magnetic absorbent to extract trace level of thrombin from dilute solutions. Finally, enriched thrombin was digested by trypsin and analyzed by matrix assisted laser desorption ionization-time of flight (MALDI-TOF) mass spectrometry. Taking advantage of the efficient affinity extraction ability of our TBA@Au-MMPs and the sensitive mass readout of MALDI-TOF, highly sensitive detection of thrombin was achieved. The limit of detection was as low as 18 fmol, corresponding to 0.36 nM thrombin in 50 μL original solution. Linear relation was observed within a concentration range from 0.5 nM to 10 nM with linear correlation $R^2 = 0.998$. Other proteins including human serum albumin (HSA), Ig G, transferrin, oval albumin (OVA) and fetal calf serum did not interfere with thrombin detection. This simple method holds great potential for analyzing, sensing, purification and preconcentration of proteins in biological fluids.

1. Introduction

Thrombin is a multifunctional serine protease that plays major roles in the coagulation cascade [1]. It is also related to a number of pathological processes, such as metastasis, cardiovascular diseases, angiogenesis, inflammation, and has been considered as a biomarker for tumor diagnosis [2–5]. The concentration of thrombin in blood can change considerably from nM to low μM levels; thrombin was reported to be remarkably overexpressed in patients with hepatocellular carcinoma [2]. Therefore, developing an assay with high sensitivity, selectivity, and simplicity for thrombin detection has great significance for the diagnosis and cure of related diseases. Li et al. [6] have developed a method for thrombin detection by a label free fluorescing molecular switch (ethidium bromide, EB). When thrombin was added, the EB molecules previously intercalated into the base pairs of the double helix of aptamer and its complementary strand was released, leading to a reduction in fluorescence intensity, and this reduction is proportional to the concentration of thrombin. However, the detection limit (2.8 nM) is not high enough and EB is a well-known mutagenic reagent that could lead to human cancer. Recently, Chen et al. [7] reported an electrochemiluminescent (ECL) method for thrombin detection using PS-$(CdTe)_n$ microbead as a new label for amplified sensitivity. CdTe quantum dots were assembled to the surfaces of polystyrene (PS) microbeads through layer-by-layer method to form PS-$(CdTe)_n$ microcomposite. The sensitivity is amplified and the detection limit is as low as 0.35 PM. However, they did not show the detection results in real serum sample and the specificity test was limited to only 2 unspecific proteins. Up to now, various methods for selective detection of thrombin using aptamer have been reported based on electrochemical methods [8–10], fluorescence methods [6,11,12], quartz crystal microbalance [13], ICP-Mass [14], and so on. However, these methods mentioned above cannot fulfill the demand in massive analysis especially in proteomic research era, for their limitations of complicated sensing mechanisms [13,15,16], laborious steps, low sensitivity [17], low analysis speed and very low-throughput [10,15,18–21]. Alternatively, MALDI-TOF mass spectrometry is a very powerful tool for the simultaneous analysis of multiple samples with high speed and sensitivity. Usually, sensitivities in femtomole range can be easily achieved. Moreover, even sensitivities in zeptomole range was

* Corresponding author. Tel.: +86 21 6564 3983; fax: +86 21 6564 1740.
E-mail address: xmzhang@fudan.edu.cn (X. Zhang).

0039-9140/$ – see front matter © 2011 Elsevier B.V. All rights reserved.
doi:10.1016/j.talanta.2011.10.044

reported [22] with microspot MALDI. Except from the unequivocal identification of a given target, MALDI-TOF has also the unparalleled ability to discriminate disease related patterns of protein post-translational modifications which cannot be revealed by the above mentioned methods [23].

Aptamers are single-stranded nucleic acids (DNA or RNA) that can bind with high affinity and specificity of a wide range of target molecules including small organic and inorganic molecules, proteins, peptides, or even living cells [24–27]. They can be selected from random libraries in vitro by a process called SELEX [28,29] (systematic evolution of ligands by exponential enrichment). Compared with conventional antibodies, aptamers offer certain advantages including low price, good stability, good reproducibility, ease of synthesis, storage, and modification [30]. There is a growing application of aptamers as antibody substitutes in immunoassays. For example, aptamers have been immobilized on graphene and graphene oxide [12,31], gold [32], nanowire [33], carbon nanotubes [34], glass slides [11], and so on.

However, to our knowledge, there are few reports using magnetic particles as the substrate for aptamer immobilization. Magnetic particles can greatly facilitate the isolation process simply by the application of a magnetic field, and have been widely applied in protein capture [35–37]. In our previous studies, we have successfully synthesized different core–shell structured magnetic microspheres and have applied them in proteomics [38–42]. To our knowledge, this is the first report of developing Au-MMPs as a substrate for TBA immobilization. Coating the surface of magnetic particles with gold layer makes them much easier for biochemical modification. Our synthesis process of Au-MMPs is based on layer-by-layer electrostatic adsorption. It is much simpler compared with current methods like iterative reduction of $HAuCl_4$ [16], reverse micelle method [43], hydroxylamine seeding [44]. Combining easy immobilization, fast separation, highly sensitive and high-throughput analysis, our method will have a bright future in automatic analysis.

2. Experimental

2.1. Chemicals and materials

The human α-thrombin binding aptamer (TBA), peptide ER-10 (ELVESYIDGR), and DF-8 (DRVYIHPF) were synthesized by Sangon Biotechnology Company (Shanghai, China). The sequence of TBA is 5′-SH-$(CH_2)_6$-TT TTT TTT TTG GTT GGT GTG GTT GG-3′ [45]. Human α-thrombin, transferrin, ovalbumin, human serum albumin (HSA), trifluoroacetic acid (TFA), α-cynano-4-hydroxycinnamic acid (CHCA) and polyelectrolyte poly (diallyldimethylammonium chloride) (PDDA), TPCK-treated trypsin were purchased from Sigma. Tris (2-carboxyethyl) phosphine hydrochloride (TCEP) was purchased from Alfa Aesar. Human serum from a healthy donor is a kind gift from Zhongshan Hospital (Shanghai, China). All the other chemicals were of analytical grade and were purchased from Shanghai Chemical Reagent Co. (Shanghai, China). All aqueous solutions were prepared with Milli-Q water (Millipore, Bedford, MA).

2.2. Synthesis of gold nanoparticles

Gold Nanoparticles (Au-NPs) were prepared according to the previous literature [46]. Briefly, 125 mL of 1 mM $HAuCl_4$ solution was added into a two-neck round-bottom flask and brought to a vigorous boil under magnetic stirring. Then, 12.5 mL of solution containing 0.143 g of trisodium citrate was added to the flask quickly. The solution turned from yellow to clear, to black, to purple to deep red. Then the solution was refluxed for another 15 min. After cooling to room temperature, the solution was filtered through 0.22 μm microporous membrane. The final gold colloid had a λ_{max} of 518 nm and the average diameter of Au-NPs was around 13 nm by TEM characterization.

2.3. Synthesis of Fe_3O_4@C magnetic microspheres

Magnetic nanoparticles were synthesized through hydrothermal reaction. Briefly, 1.35 g of $FeCl_3{\cdot}6H_2O$ was first dissolved in 75 mL of ethylene glycol under magnetic stirring. A clear orange solution was obtained after stirring for 0.5 h. Then 3.60 g of sodium acetate was added to this solution. After stirring for another 0.5 h, the resulting solution was transferred into a Teflon-lined stainless-steel autoclave with a capacity of 200 mL. The autoclave was sealed and heated at 200 °C for 16 h and then cooled to room temperature. The magnetic microspheres were collected with the help of a magnet, followed by washing with ethanol and deionized water six times. The product was then dried under vacuum at 50 °C for 5 h.

In the next step, 0.2 g of magnetic microspheres was ultrasonicated for 10 min in 0.1 M HNO_3, followed by washing with deionized water for three times. After that, the treated Fe_3O_4 microspheres were re-dispersed in 0.5 M aqueous glucose solution and ultrasonicated for another 10 min. Then the suspension was transferred to autoclave and kept at 180 °C for 6 h and cooled to room temperature. The microspheres were isolated with the help of a magnet and washed with ethanol six times. At last, the Fe_3O_4@C microspheres were dried under vacuum at 50 °C for 5 h.

2.4. Synthesis of Au-MMPs

60 mg of Fe_3O_4@C magnetic microspheres were dispersed into an aqueous solution of 0.20% PDDA that contained 20 mM Tris base and 20 mM NaCl. The resulting dispersion was stirred for 20 min. PDDA adsorbed microspheres were collected with the help of a magnet and rinsed with water six times. The resulting magnetic microspheres were re-dispersed in 100 mL of gold colloid solution and the mixture was stirred for another 20 min. The supernatant was removed with the help of a magnet. The obtained Au-MMPs magnetic microspheres were washed with deionized water three times and dried under vacuum at 50 °C for 6 h.

2.5. Preparation of TBA@ Au-MMPs

4 nmol of SH-TBA was incubated with 2.5 mM of TCEP (pH 5.0) in dark for an hour in order to break the disulfide bond formed between two DNA chains. Then as-prepared solution was transferred to an Eppendorf tube containing 15 mg of Au-MMPs magnetic microspheres. The reaction continued for 12 h in dark under vigorous shaking. Next, remove the supernatant with the help of a magnet and wash the microspheres with Tris–acetate buffer (50 mM Tris base, 100 mM NaCl, pH 8.0) three times. At last, store the TBA functionalized Au-MMPs magnetic microspheres in Tris–acetate buffer at 4 °C. The immobilization efficiency was calculated according to absorption differences at 260 nm.

2.6. Protein capture and analysis

TBA exists in solution in a balance between two forms, the random structure and G-quadruplex structure, and the G-quadruplex structure is able to bind thrombin with high affinity and specificity. Potassium ions (K^+) are known to stabilize the G-quadruplex structure [47]. The binding buffer is PBS (137 mM NaCl, 2.7 mM KCl, 10 mM Na_2HPO_4, 2 mM KH_2PO_4). Proteins dissolved in PBS buffer were incubated with TBA@Au-MMPs magnetic microspheres and stirred under room temperature for 1 h. After incubation, the microspheres were washed with PBS three times to remove any unbound or weakly bound species, and 25 mM NH_4HCO_3 buffer three times

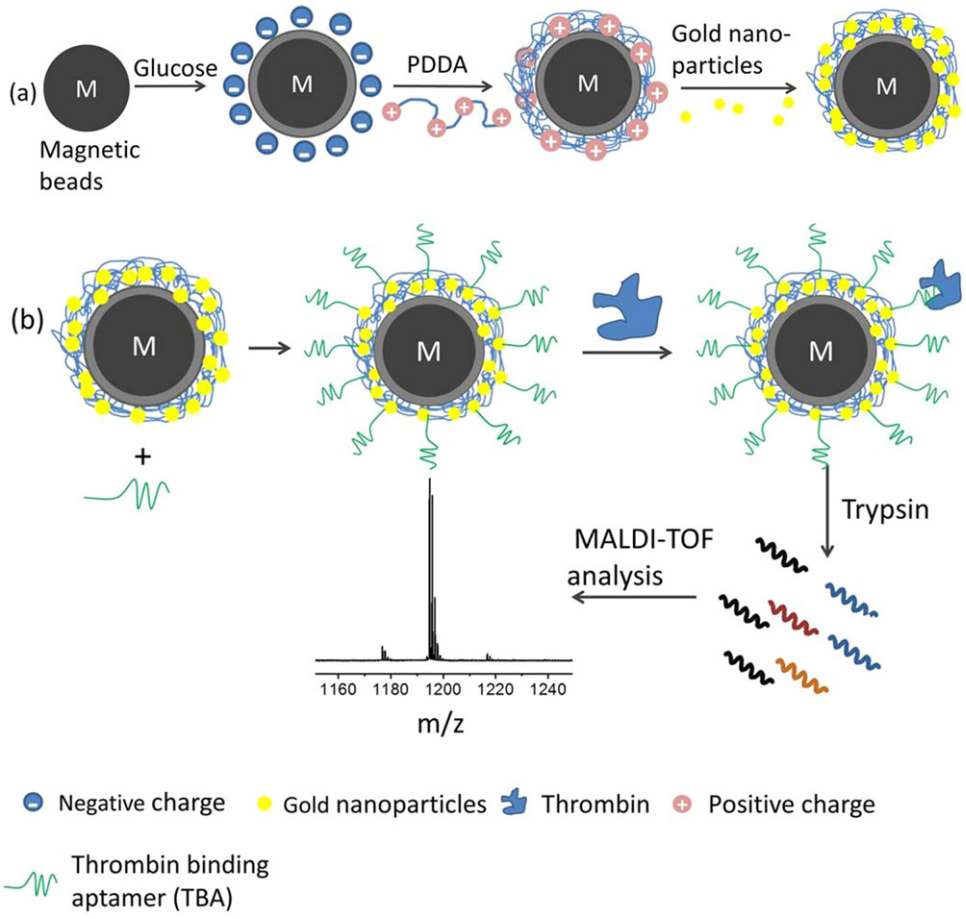

Scheme 1. (a) Schematic diagram representation of the synthesis process of core–shell structure Au-MMPs. (b) Schematic diagram representation of thrombin detection using core–shell Au-MMPs, TBA, and MALDI-TOF mass spectrometry. Thrombin was first captured by TBA@Au-MMPs. Then after trypsin digestion, the intensity of MALDI-TOF analysis at *m*/*z* of 1194.6, which is a peptide belongs to thrombin with sequence ELLESYIDGR, corresponded to the original concentration of thrombin.

to adjust the pH for trypsin digestion. Then, microspheres were reconstituted with NH_4HCO_3 buffer and heated at 100 °C for 1 min. Next, trypsin was added and the mixture was digested overnight at 37 °C. Add 20 pg of peptide DF-8 or 200 pg of peptide ER-10 as the internal standard to the suspension after digestion. Finally, 1 μL of supernatant and 0.5 μL of CHCA matrix solution (4 mg/mL, 0.1% TFA in 50% ACN/H_2O solution) was spotted on a MALDI target plate for mass spectrometry analysis.

2.7. MALDI-TOF mass analysis

Positive ion MALDI-TOF mass spectrometry spectra were acquired on AB SCIEX TOF/TOF 5800 (Applied Biosystems). The sample was excited using an Nd: YAG laser (355 nm) operated at a repetition rate of 400 Hz and acceleration voltage of 20 kV. The MS instrument was calibrated with tryptic peptides of myoglobin. The MASCOT server was used to interpret the MALDI-TOF/TOF mass spectrometry data by searching in the NCBI database.

3. Results and discussion

3.1. Preparation and characterization of Au-MMPs magnetic microspheres

The synthesis process of core–shell Au-MMPs is shown in Scheme 1(a). At first, magnetic (Fe_3O_4) microspheres were synthesized via hydrothermal reaction. Then it was coated with hydrophilic carbon by hydrothermal reaction of glucose to form core–shell structured magnetic microspheres with uniform carbonaceous layer (Fe_3O_4@C). The hydrophilic surface of Fe_3O_4@C can greatly reduce nonspecific adsorptions. The combination of Au nanoparticles to composite Fe_3O_4@C is based on layer-by-layer electrostatic adsorption. Basically, Fe_3O_4@C microspheres bear negative charges. In order to adsorb negatively charged Au nanoparticles, we modified them with PDDA, which provide a homogeneous distribution of positive charges over the carbonaceous shell. SEM and TEM were employed to investigate the structure of the as-synthesized core–shell Au-MMPs (Fig. 1). In SEM image, Au-MMPs look like “nano-waxberry”, the surface of which were full of nano-granules due to the existence of gold nanoparticles. It is also very clear to see from TEM images that the magnetic core was totally warped by a condense layer of gold nanoparticles, providing it an excellent substrate for biochemical modification. Au-S covalent bond formation is a one-step reaction. The immobilization of TBA on Au-MMPs is much easier compared with other nanoparticles, nanofibers, or microchips, which usually have functional groups like amine, carboxyl, or hydroxyl groups. For example, to successfully conjugate aptamers on amine or carboxyl group containing surface, EDC (1-ethyl-3-(3-dimethylaminopropyl) carbodiimide) and NHS (N-hydroxysuccinimide) are the most popular crosslinking reagent pair. However, this is a two-step reaction and hard to complete because EDC is easy to hydrolysis and lose its function in water [48]. In another hand, hydroxyl groups are more difficult than amine groups to be conjugated. Usually the activation of hydroxyl groups relies on silanization reaction to introduce amine, epoxide, thiol group and so on [49].

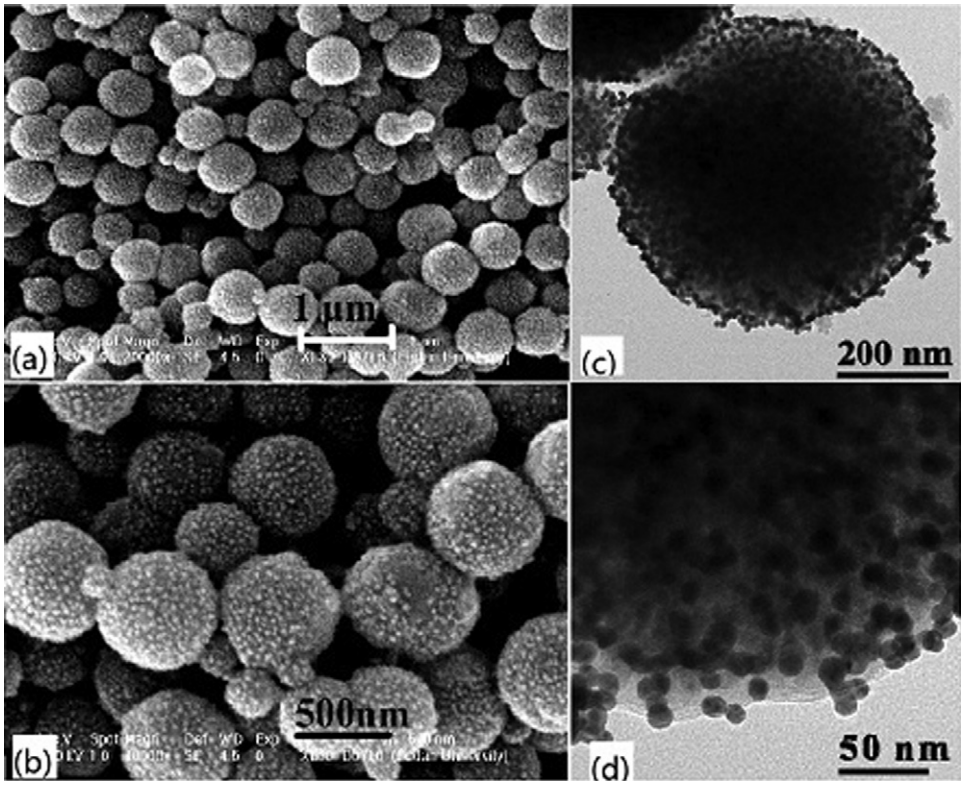

Fig. 1. SEM ((a) and (b)) and TEM ((c) and (d)) images of Au-MMPs, which show clearly numerous small Au nanoparticles, were deposited on to the surface of magnetic microspheres.

Another choice for aptamer immobilization was based on the strong interaction between avidin and biotin. Usually avidin is immobilized on the support through its amine functional group and aptamer is biotin modified. However, adding a biotin group at one end of aptamer could possibly deteriorate the binding affinity of the aptamer [50]. In one sentence, the immobilization of aptamer on Au-MMPs is very easy and efficient, and the magnetic nature can facilitate a fast separation which is very important for speedy analysis nowadays. The preparation of Au-MMPs is highly reproducible. The amount of TBA immobilized on Au-MMPs was averaged to be 0.15 ± 0.015 nmol/mg of microspheres in five repetitive experiments with freshly prepared Au-MMPs by UV absorption measurement at 260 nm.

3.2. Thrombin enrichment and optimization of experimental conditions

In order to test the feasibility of our method on thrombin detection, the analysis of 50 μL of bulk solutions with thrombin concentration at 250 nM was performed. Thrombin solution was incubated with TBA@Au-MMPs for an hour. The magnetic nature of our TBA@Au-MMPs facilitated a fast separation of captured thrombin from the sample mixture and the excess reagents. Then, TBA@Au-MMPs were washed with PBS and 25 mM NH_4HCO_3 buffer for three times to remove any unbound or weakly bound species. After that, microspheres were reconstituted with 2 μL of NH_4HCO_3 buffer. This small volume was applied to keep sample concentrated during the following process of trypsin digestion and MALDI-TOF analysis. Trypsin was chosen as the enzyme for digestion due to its ability to generate peptides with moderate length suitable for mass analysis. We added trypsin directly to the thrombin enriched TBA@Au-MMPs without performing any elution step. This is time-saving, and the potential sample loss due to incomplete elution and sample manipulation, which is detrimental especially for trace level of sample, is totally avoided. Fig. 2 shows a typical MALDI-TOF mass spectrum. Among the whole mass range from 900 Da to 2500 Da, the peak of m/z 1194.6 is the strongest. The intensities of most other peaks in the spectrum are very low. Upon the binding of TBA and thrombin, some proteolytic sites may be blocked by TBA and/or microsphere. By tandem MS analysis and database searching we have confirmed that peak 1194.6, with sequence ELLESYIDGR, did belong to thrombin. So we chose peak 1194.6 as the signal peptide.

The amount of Au-MMPs greatly influences the final intensity of the signal peptide. An excess of TBA can lead to a better recovery of thrombin from dilute solutions. But the mass signal intensity may diminish due to nonspecific adsorption of peptides when microspheres are too much. We observed significant signal decrease and noise increment if microspheres used were more than 333 μg

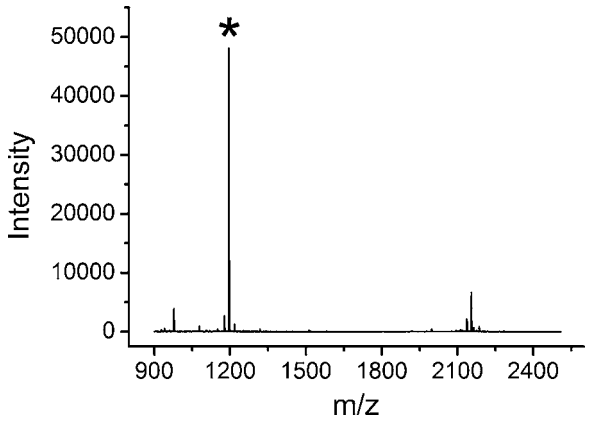

Fig. 2. Typical MALDI-TOF mass spectra obtained after enrichment and trypsin digestion of thrombin at 250 nM. Black asterisk represents signal peptide (m/z = 1194.6), which is the strongest peak detected in the mass range from 900 Da to 2500 Da.

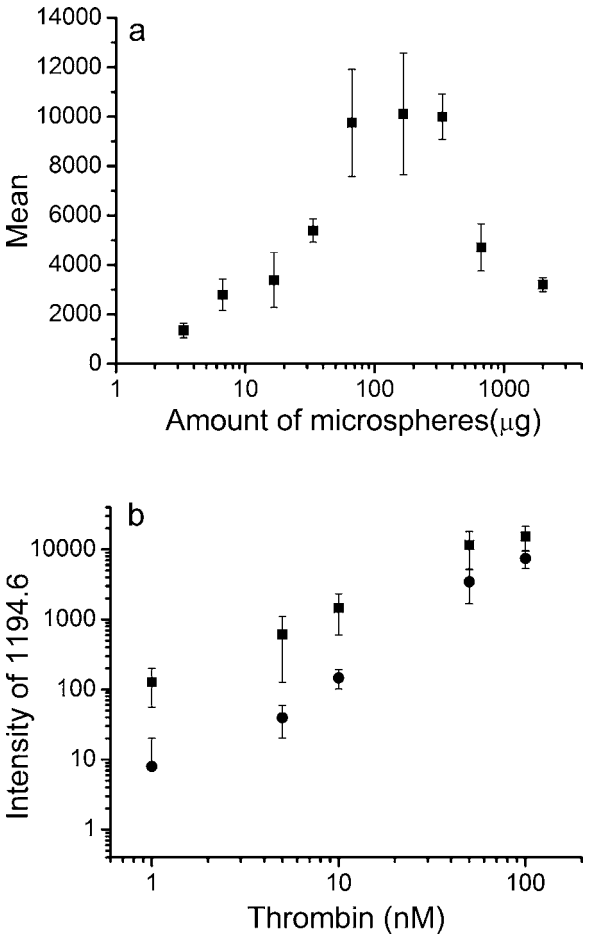

Fig. 3. (a) Influence of the amount of microspheres on mass intensity of signal peptide. Thrombin concentration: 100 nM; (b) Influence of heat denaturing before digestion to the signal intensity. Squares: with heat denaturing; circles: without heat denaturing.

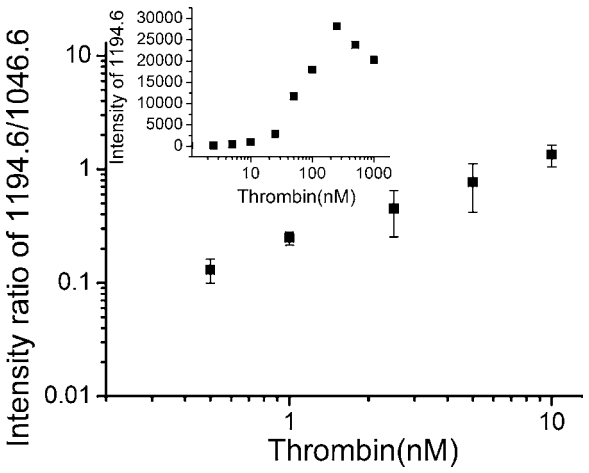

Fig. 4. The calibration curve. Linear relation was observed within a concentration range of 0.5–10 nM with linear correlation $R^2 = 0.998$ in the 50 μL original standard solution. The results were averaged from 3 replicate analyses. The inset shows the intensity of signal peptide in concentration range from 0.5 nM to 1000 nM. The signal suffered a great reduction when concentration was larger than 250 nM.

under our experimental conditions. Fig. 3(a) shows that the signal reaches a short plateau when the amount of microspheres is in the range from 66 μg to 333 μg, which corresponds to TBA range from 10 pmol to 50 pmol. Thus we chose 66 μg in all our following experiments.

By heating the thrombin entrapped microspheres at 100 °C for 1 min the mass signal of peptide 1194.6 increased significantly (Fig. 3(b)). Both of the three-dimensional structure of TBA and thrombin were partially disrupted by this high temperature, leading to the release of thrombin and exposure of more proteolytic sites.

3.3. Calibration curve and detection limit

To test whether our method could quantitatively measure thrombin, we constructed a calibration curve by measuring the

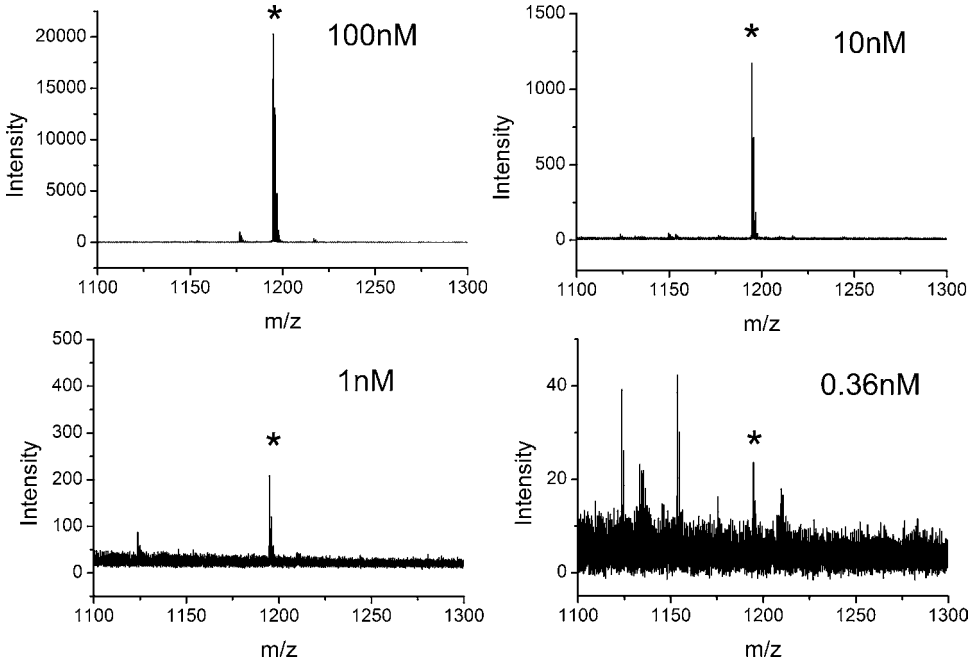

Fig. 5. Signal intensities under different concentrations of thrombin. Black asterisk represents the position of signal peptide. The detection limit was calculated to be 0.36 nM based on three times standard deviation of blanks and the calibration curve.

intensity of signal peptide from a series of dilutions of thrombin from 0.5 nM to 1000 nM. Peptide DF-8 (m/z = 1046.6) with sequence DRVYIHPF was added as the internal standard. When concentration of thrombin was larger than 250 nM, the intensity of signal peptide began to drop quickly (Fig. 4, inset). Three replicate analyses yielded a good linear response (R^2 = 0.998) in thrombin concentration range from 0.5 nM to 10 nM (Fig. 4). The linear regression is $Y = 0.7556X - 0.6346$, where Y stands for the logarithm of intensity ratio of 1194.6 versus 1046.6, X stands for the logarithm of concentration of thrombin in nM. By using the calibration curve and three times standard deviation of blanks, limit of detection was calculated to be 0.36 nM, corresponding to 18 fmol in 50 μL original solution. The detectability of our method when thrombin concentration was as low as 0.36 nM was evaluated. Fig. 5 shows mass intensities of signal peptide under different concentrations of thrombin, including that of 0.36 nM. Under this concentration, the signal-to-noise ratio (S/N) was determined to be larger than 10 by Data Explorer (TM) Software.

3.4. Specificity test

We further tested the specificity of our method for detection of thrombin. Four other proteins and fetal calf serum were tested in place of thrombin, using the exact same experimental procedures as those for thrombin. All the experiments were repeated for three times. The concentrations of other standard proteins were 100 nM for transferrin, Ig G, HSA, and OVA. Fetal calf serum was thawed from −20 °C and used after centrifugation at 4 °C for 20 min to remove any insoluble component. The mass signal intensities at m/z of 1194.6 were considered as the response to different proteins and plotted on y-axis. Fig. 6 shows that 10-fold excess of transferrin, Ig G, HSA, and OVA and even fetal calf serum did not interfere with the determination for a trace level (10 nM) of thrombin.

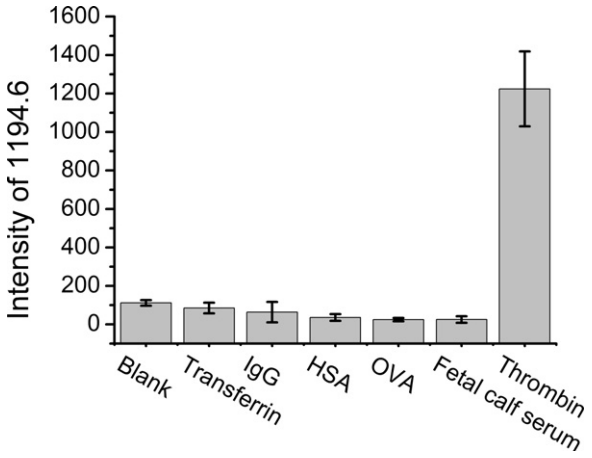

Fig. 6. The specificity test. Test the response of 10-fold excess of four other proteins, and fetal calf serum in 50 μL original solution. Thrombin concentration: 10 nM.

3.5. Thrombin detection in human serum

Because the detection of thrombin in serum or blood is clinically relevant, the practicality of using our assay for this purpose was tested. Human serum was thawed from −80 °C and centrifuged at 4 °C for 20 min to remove any insoluble component. Before

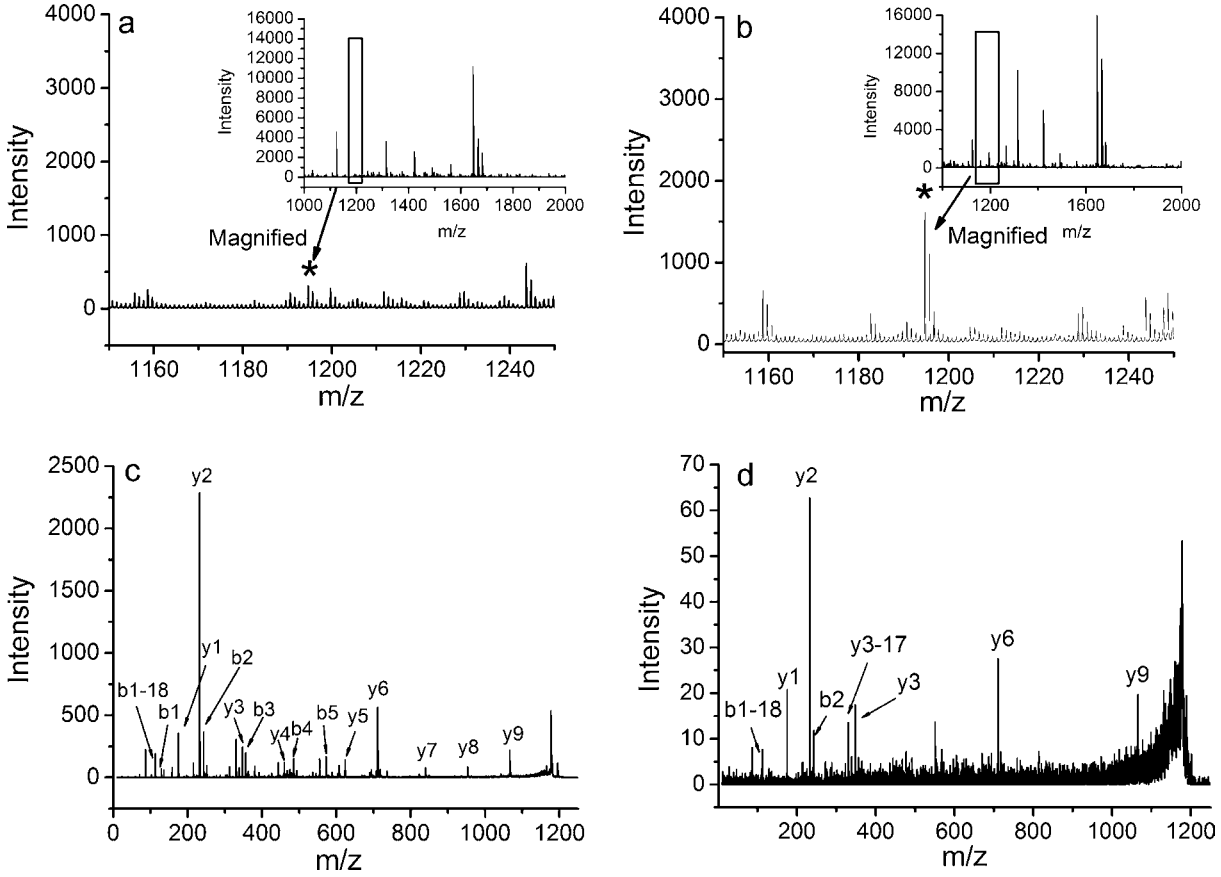

Fig. 7. Thrombin detection in human serum. Black asterisk represents the position of signal peptide. (a) 10-fold-diluted human serum without addition of thrombin; (b) Thrombin was added to 10-fold-diluted human serum with a fixed final concentration of 10 nM; (c) standard MS/MS spectrum of signal peptide required from thrombin standard solutions showing y-ions and b-ions; (d) MS/MS spectrum of signal peptide in (b).

Table 1
The recovery of thrombin from human serum, $C_{thrombin}$=10 nM.

Internal standard	Dilution fold	Detected concentration	Recovery
ER-10	5 fold	16.7 ± 0.9 nM	167 ± 9%
	10 fold	10.2 ± 0.5 nM	102 ± 5%
	20 fold	11.4 ± 1.0 nM	114 ± 10%
	50 fold	11.6 ± 1.1 nM	116 ± 11%
DF-8	5 fold	23.8 ± 1.1 nM	238 ± 11%
	10 fold	15.1 ± 0.4 nM	151 ± 4%
	20 fold	14.5 ± 0.9 nM	145 ± 9%
	50 fold	14.1 ± 1.0 nM	141 ± 10%

analysis, serum samples were diluted 10 fold with PBS buffer. Dilution is a common adopted pretreatment procedure for protein detection in sample of high complexity such as human serum [13,14,51–53]. To the diluted serum was either added or not 500 fmol of thrombin to ensure a final concentration of 10 nM. Then, same experimental procedures as those for the thrombin standard were adopted. In the case that serum was analyzed without adding thrombin, signal of peptide 1194.6 was barely discernable because the endogenous level of thrombin in healthy human serum is very low (Fig. 7(a)). When 10 nM of thrombin was added (Fig. 7(b)), peak 1194.6 became quite distinctive with a high response that was comparable to that of standard solutions (Fig. 5, upright). The MS/MS analysis to signal peptide was also performed, and the result is shown in Fig. 7(d). By comparing the ion pattern with that obtained from thrombin stand solutions (Fig. 7(c)) the successful detection of thrombin was further confirmed. In Fig. 7(a) and (b), there exist certain background peaks in the spectrum. However, this is not surprising because some background peaks will always be present from complex samples such as human serum [53]. What's interesting is that, none of the three most commonly found high-abundance proteins including HSA, Ig G, and transferrin were identified in these background peaks by further tandem mass analysis and database searching. Alternatively, we have confirmed proteins including vitronectin, histidine rich glycoprotein, complement C3, apolipoprotein E, and isocitrate dehydrogenase [NADP] cytoplasmic (data not shown). The common levels of these proteins in human serum are much lower than that of albumin, transferrin and Ig G [54]. The reason behind is still under exploration. We suspect that the surface charges carried by our Au-MMPs would induce certain background peaks. And protein–protein interaction may also lead to further adsorption of related proteins.

The recovery of thrombin from human serum was evaluated and the result is shown in Table 1. Unfortunately, the ion intensity of our internal standard peptide DF-8 was severely suppressed in the spectrum and leading to recoveries even larger than 200%. Another internal standard ER-10 was added for comparison. The sequences of ER-10 (EL**V**ESYIDGR) and 1194.6(EL**L**ESYIDGR) differ by only one amino acid (highlighted). Structural analog is a good choice as internal standard sometimes as reported in reference [55]. The performance of structural analog ER-10 in serum is much better than DF-8. Although the recoveries at 5 fold dilution were much larger than 100% for both internal standards, the recoveries began to decline with increasing of dilution fold. And specifically, when ER-10 was used and the dilution was more than 10 fold, the recoveries were quite close to 100%. Internal standard selection is critical and stable isotopomers are still the best choice for eliminating ion suppression effect [55,56].

4. Conclusions

In this work, Au-MMPs were developed as a novel substrate for aptamer immobilization. Simple, rapid and sensitive thrombin detection was achieved. Aptamers are very stable; they could be stored for months without any loss of activity. Beyond thrombin detection, extended application of affinity capture of other proteins, peptides and small molecules can be achieved as long as they have corresponding aptamers. Given the versatile assay design, stable affinity probe, simple analytical procedure and high speed and sensitive MALDI-TOF analysis, our newly developed methodology is useful for rapid target detection, characterization of protein modification, and other applications in clinical proteomics.

Acknowledgements

This work was supported by the National Key Natural Science Foundation of China (Project: 21027002), the National Basic Research Priorities Program (2007CB914100) and Shanghai Leading Academic Discipline Project (B109).

References

[1] A.S. Wolberg, Blood Rev. 21 (2007) 131.
[2] Y.H. Xue, X.F. Zhang, Q.Z. Dong, J.A. Sun, C. Dai, H.J. Zhou, N. Ren, H.L. Jia, Q.H. Ye, L.X. Qin, Hepatology 52 (2010) 2012.
[3] E. Dupuy, A. Habib, M. Lebret, R. Yang, S. Levy-Toledano, G. Tobelem, J. Thromb. Haemost. 1 (2003) 1096.
[4] M.L. Nierodzik, S. Karpatkin, Cancer Cell 10 (2006) 355.
[5] N.E. Tsopanoglou, M.E. Maragoudakis, Eur. Cytokine Netw. 20 (2009) 171.
[6] B.L. Li, H. Wei, S.J. Dong, Chem. Commun. (2007) 73.
[7] Y. Chen, B.Y. Jiang, Y. Xiang, Y.Q. Chai, R. Yuan, Chem. Commun. 47 (2011) 7758.
[8] A.V. Porfireva, G.A. Evtugyn, A.N. Ivanov, T. Hianik, Electroanalysis 22 (2010) 2187.
[9] Z. Jing, G.F. Cheng, P.G. He, Y.Z. Fang, Talanta 80 (2010) 1868.
[10] A. Numnuam, K.Y. Chumbimuni-Torres, Y. Xiang, R. Bash, P. Thavarungkul, P. Kanatharana, E. Pretsch, J. Wang, E. Bakker, Anal. Chem. 80 (2008) 707.
[11] D.W. Huang, C.G. Niu, P.Z. Qin, M. Ruan, G.M. Zeng, Talanta 83 (2010) 185.
[12] H.X. Chang, L.H. Tang, Y. Wang, J.H. Jiang, J.H. Li, Anal. Chem. 82 (2010) 2341.
[13] Q.A. Chen, W. Tang, D.Z. Wang, X.J. Wu, N. Li, F. Liu, Biosens. Bioelectron. 26 (2010) 575.
[14] Q. Zhao, X.F. Lu, C.G. Yuan, X.F. Li, X.C. Le, Anal. Chem. 81 (2009) 7484.
[15] B. Wang, C. Yu, Angew. Chem.-Int. Edit. 49 (2010) 1485.
[16] G. Liang, S. Cai, P. Zhang, Y. Peng, H. Chen, S. Zhang, J. Kong, Anal. Chim. Acta 689 (2011) 243.
[17] C.M. Wang, M. Hossain, L.Y. Ma, Z.Y. Ma, J.J. Hickman, M. Su, Biosens. Bioelectron. 26 (2010) 437.
[18] J.A. Hansen, J. Wang, A.N. Kawde, Y. Xiang, K.V. Gothelf, G. Collins, J. Am. Chem. Soc. 128 (2006) 2228.
[19] K.A. Edwards, Y. Wang, A.J. Baeumner, Anal. Bioanal. Chem. 398 (2010) 2645.
[20] J. Huang, Z. Zhu, S. Bamrungsap, G.Z. Zhu, M.X. You, X.X. He, K.M. Wang, W.H. Tan, Anal. Chem. 82 (2010) 10158.
[21] J.L. Wang, A. Munir, H.S. Zhou, Talanta 79 (2009) 72.
[22] B.O. Keller, L. Li, J. Am. Soc. Mass Spectrom. 12 (2001) 1055.
[23] K.Y. Wang, S.A. Chuang, P.C. Lin, L.S. Huang, S.H. Chen, S. Ouarda, W.H. Pan, P.Y. Lee, C.C. Lin, Y.J. Chen, Anal. Chem. 80 (2008) 6159.
[24] Z. Zhu, C.C. Wu, H.P. Liu, Y. Zou, X.L. Zhang, H.Z. Kang, C.J. Yang, W.H. Tan, Angew. Chem.-Int. Edit. 49 (2010) 1052.
[25] X.H. Fang, W.H. Tan, Accounts Chem. Res. 43 (2010) 48.
[26] E.W.M. Ng, D.T. Shima, P. Calias, E.T. Cunningham, D.R. Guyer, A.P. Adamisv, Nat. Rev. Drug Discov. 5 (2006) 123.
[27] J. Ciesiolka, M. Yarus, RNA-Publ. RNA Soc. 2 (1996) 785.
[28] A.D. Ellington, J.W. Szostak, Nature 346 (1990) 818.
[29] C. Tuerk, L. Gold, Science 249 (1990) 505.
[30] S.M. Nimjee, C.P. Rusconi, B.A. Sullenger, Annu. Rev. Med. 56 (2005) 555.
[31] B. Gulbakan, E. Yasun, M.I. Shukoor, Z. Zhu, M.X. You, X.H. Tan, H. Sanchez, D.H. Powell, H.J. Dai, W.H. Tan, J. Am. Chem. Soc. 132 (2010) 17408.
[32] Y.C. Shiang, C.C. Huang, T.H. Wang, C.W. Chien, H.T. Chang, Adv. Funct. Mater. 20 (2010) 3175.
[33] X. Luo, I. Lee, J. Huang, M. Yun, X.T. Cui, Chem. Commun. 47 (2011) 6368.
[34] K. Maehashi, T. Katsura, K. Kerman, Y. Takamura, K. Matsumoto, E. Tamiya, Anal. Chem. 79 (2006) 782.
[35] J. Lu, D.W. Qi, C.H. Deng, X.M. Zhang, P.Y. Yang, Nanoscale 2 (2011) 1892.
[36] H.M. Chen, S.S. Liu, Y. Li, C.H. Deng, X.M. Zhang, P.Y. Yang, Proteomics 11 (2011) 890.
[37] J. Tang, Y. Liu, P. Yin, G.P. Yao, G.Q. Yan, C.H. Deng, X.M. Zhang, Proteomics 10 (2010) 2000.
[38] H.M. Chen, C.H. Deng, Y. Li, Y. Dai, P.Y. Yang, X.M. Zhang, Adv. Mater. 21 (2009) 2200.
[39] H.M. Chen, C.H. Deng, X.M. Zhang, Angew. Chem.-Int. Edit. 49 (2010) 607.
[40] S.S. Liu, H.M. Chen, X.H. Lu, C.H. Deng, X.M. Zhang, P.Y. Yang, Angew. Chem.-Int. Edit. 49 (2010) 7557.
[41] G.P. Yao, C.H. Deng, X.M. Zhang, P.Y. Yang, Angew. Chem.-Int. Edit. 49 (2010) 8185.

[42] D.W. Qi, H.Y. Zhang, J. Tang, C.H. Deng, X.M. Zhang, J. Phys. Chem. C 114 (2010) 9221.
[43] S.J. Cho, J.C. Idrobo, J. Olamit, K. Liu, N.D. Browning, S.M. Kauzlarich, Chem. Mat. 17 (2005) 3181.
[44] J.L. Lyon, D.A. Fleming, M.B. Stone, P. Schiffer, M.E. Williams, Nano Lett. 4 (2004) 719.
[45] H. Yang, J. Ji, Y. Liu, J.L. Kong, B.H. Liu, Electrochem. Commun. 11 (2009) 38.
[46] H.D. Hill, C.A. Mirkin, Nat. Protoc. 1 (2006) 324.
[47] A.H. Liang, J.S. Li, C.N. Jiang, Z.L. Jiang, Bioprocess. Biosyst. Eng. 33 (2010) 1087.
[48] G.T. Hermanson, Pierce Biotechnology, Elsevier, Thermo Fisher Scientific, Rockford, IL, USA, 2008.
[49] D. Li, W.Y. Teoh, J.J. Gooding, C. Selomulya, R. Amal, Adv. Funct. Mater. 20 (2010) 1767.
[50] N. Tuleuova, N.C. Jones, J. Yan, E. Ramanculov, Y. Yokobayashi, A. Revzin, Anal. Chem. 82 (2010) 1851.
[51] C.K. Chen, C.C. Huang, H.T. Chang, Biosens. Bioelectron. 25 (2010) 1922.
[52] X.Y. Wang, J.M. Zhou, W. Yun, S.S. Xiao, Z. Chang, P.G. He, Y.Z. Fang, Anal. Chim. Acta 598 (2007) 242.
[53] H. Yan, A. Ahmad-Tajudin, M. Bengtsson, S. Xiao, T. Laurell, S. Ekström, Anal. Chem. 83 (2011) 4942.
[54] G.L. Hortin, D. Sviridov, N.L. Anderson, Clin. Chem. 54 (2008) 1608.
[55] E. Szajli, T. Feher, K.F. Medzihradszky, Mol. Cell. Proteomics 7 (2008) 2410.
[56] M. Bucknall, K.Y.C. Fung, M.W. Duncan, J. Am. Soc. Mass Spectrom. 13 (2002) 1015.